RSC Advances

Enhanced microwave absorption of flower-like FeNi@C nanocomposites by dual dielectric relaxation and multiple magnetic resonance

Journal:	*RSC Advances*
Manuscript ID:	RA-ART-02-2014-001437.R1
Article Type:	Paper
Date Submitted by the Author:	15-Apr-2014
Complete List of Authors:	Feng, Chao; School of Materials Science and Engineering, Anhui University of technology Liu, Xianguo; Institute of Metal Research, Shenyang National Laboratory for Material Science Sun, Yuping; Center for Engineering practice and Innovation Education, Anhui University of technology Jin, Chuangui; School of Materials Science and Engineering, Anhui University of technology Lv, Yaohui; School of Materials Science and Engineering,

Cite this: DOI: 10.1039/c0xx00000x

www.rsc.org/advances

PAPER

Enhanced microwave absorption of flower-like FeNi@C nanocomposites by dual dielectric relaxation and multiple magnetic resonance

Chao Feng,[a] Xianguo Liu,*[a] Yuping Sun,*[b] Chuangui Jin,[a] and Yaohui Lv[a]

Received (in XXX, XXX) Xth XXXXXXXXX 20XX, Accepted Xth XXXXXXXXX 20XX

DOI: 10.1039/b000000x

Flower-like FeNi@C nanocomposites self-assembled by FeNi nanosheets and flocculent carbon were synthesized by the hydrothermal method. The electromagnetic parameters of FeNi@C-paraffin composites were measured at 0.03-18 GHz. Dual dielectric relaxations in the composites system, due to the cooperative consequence of the FeNi-C interfaces and the dielectric carbon. The strong magnetic loss is from the coexistence of natural resonance and exchange resonance. For 2.0 mm thickness layer, an optimal reflection loss (RL) of -46.7 dB is observed at 3.17 GHz. The absorbent with a thickness of 1.3 mm has a RL of -32.78 dB at 13.78 GHz. The excellent microwave absorption abilities results from the synergy of dielectric loss and magnetic loss and the quarter-wavelength cancellation.

1. Introduction

The rapid development of wireless communications and high frequency circuit devices is increasingly drawing attention and interest to the study of electromagnetic (EM) wave absorption materials.[1-3] Among the candidates for EM wave absorption materials, soft magnetic ferrites have been used as the most popular conventional magnetic fillers because of their relatively high resistivity. However, the relative low saturation magnetization and low Curie temperature and negative thermal coefficient of resistivity lead to the poor EM absorption properties.[4] Metal-based absorbers are susceptible to corrosion in harsh environments (e.g., high-temperature, high-humidity, and acidic environments) that severely deteriorate the absorption performance.[5] The EM absorbing characteristics can be effectively evaluated by the relative complex permittivity ($\varepsilon_r = \varepsilon' - j\varepsilon''$) and permeability ($\mu_r = \mu' - j\mu''$),in which the real and imaginary parts represent the storage and loss of EM wave energy in absorbents through various magnetic and/or dielectric phenomena, respectively.[6] Optimization of the permeability and permittivity, so-called the EM impedance matches, which is critical for the improvement of EM wave absorbent, can be achieved by compositing magnetic and dielectric components.[7-9] Furthermore, according to the transmission line theory, the value of permittivity should be close to that of permeability in order to obtain the desired impedance match.[10] Core-shell structured magnetic nanocomposites which are provided with permittivity and permeability in one nanosystem, displays low density and good microwave absorption performance. A number of nanocomposites with core-shell structure, like FeCo/Al_2O_3, Fe/C, Ni/C, Fe/SnO, and $FeNi_3$/C, have been prepared and their EM absorbing performances have been studied.[1, 11-14] However, due to the relative low permeability (~ 1) at GHz frequency range, this type absorber just exhibits excellent EM properties in limited frequency and is sensitive to the absorbing thickness and frequency, which become the challenge for high technological applications.[15]

Permeability values of traditional microwave magnetic materials are small in frequencies of gigahertz due to Snoek's limit.[16] However, by introducing an easy magnetization plane, the intrinsic high frequency property could be enlarged greatly compared with the materials constrained by the traditional Snoek's limit.[16] The EM wave absorbers filled by flake-shaped metallic magnetic particles, such as Fe, FeNi, and FeSiAl flake-shaped particles, have attracted much attention during recent years.[17-20] Because it has particle size (in plane) at micrometer scale and thickness at nanometer size. Surface anisotropy and exchange energy, which are essential for nanostructure, are considered to root in nanoparticles with each single flake. As the magnetic moments lie in the flake plane, the product of initial susceptibility and natural resonance frequency can exceed Snoek's limit and hence the flake-shaped particles can possess high permeability in GHz range.[21]

FeNi alloys are one of the most widely used soft magnetic materials due to their high saturation magnetization (MS), high permeability, high Curie temperature and low energy losses, which are widely used in EM wave absorbers, antennas, magnetic sensors and actuators, catalyst, and magnetic recording systems, etc.[22,23] Carbon-based materials, with high chemical and thermal stabilities, high mechanical properties, low density, high electric resistivity and permittivity, are good dielectric loss absorbers, while the relatively low permeability limits its potential applications for EM absorbing materials. Carbon/ferromagnet composites have better balance between permittivity and permeability than individual magnet or carbon absorber.[24-26] Integrating nanoscale FeNi alloys with carbon will combine the excellent properties of both of them into one nano-system, which promises many practical applications in future nanotechnology.

In this work, a new type of flower-like FeNi@C composite, which are self assembled by FeNi nanosheet and flocculent-like carbon, has been developed. The morphology and microstructure of flower-like FeNi@C composite is investigated. The FeNi@C-paraffin composites are fabricated and their microwave EM properties are studied. The dependence of reflection loss (RL) peak frequency on absorber thickness has been deeply investigated from viewpoint of their origin.

2. Experimental

2.1 Materials

All the reactants, $Ni(NO_3)_2{\cdot}6H_2O$, $Fe(NO_3)_2{\cdot}9H_2O$, hydrazine hydrate ($N_2H_4{\cdot}H_2O$), sodium dodecyl sulfate (SDS), NaOH and glucose are obtained from Shanghai Chemical Company (Shanghai, China). All chemicals are of analytical grade and used without further purification. Distilled water obtained from Milli-Q system (Millipore, Bedford, MA) is used in all experiments.

2.2 Synthesis of flower-like FeNi nanostructures

The synthesis of flower-like FeNi nanocomposites was performed in a 50-mL Teflon-lined stainless steel autoclave. In a typical experiment, a solution was first prepared by dissolving $Ni(NO_3)_2{\cdot}6H_2O$ and $Fe(NO_3)_2{\cdot}9H_2O$ in distilled water in amounts corresponding to the molar ratio of nickel to iron of 1:1. Subsequently, some NaOH was added to the solution to keep its pH around 11. A 2 mL volume of $N_2H_4{\cdot}H_2O$ as reluctant was added to the solution, and 0.5 mL of SDS was used as surfactant. The mixture was stirred vigorously until it was homogeneous and then was transferred into an autoclave. The autoclave was sealed and put into a furnace, which was preheated to 160 ^oC. After heating for 10 h, the autoclave was taken out and cooled naturally to room temperature. The product was washed with distilled water and ethanol several times to remove impurities.

2.3 Preparation of flower-like FeNi@C nanocomposites

The above black products were dissolved in 40 ml distilled water with 2 g glucose. The mixture was automatically stirred for 30 min and then was transferred into a 50 ml autoclave. The autoclave was sealed and put into a furnace with the temperature of 140 ^oC. After heating for 8 h, the autoclave was cooled naturally to room temperature. The product was washed with distilled water and ethanol several times to remove impurities before the characterizations.

2.4 Characterization

The composition and phase purity of the as-prepared sample were analyzed by X-ray diffraction (XRD, Brucker D8 Advance, Germany) at a voltage of 40 kV voltage and a current of 50 mA with Cu Kα radiation (λ=1.5418 Å). Scanning electron microscopy (SEM) was performed using JEOL-6300 F (Japan) scanning electron microscopy equipped with energy dispersive spectrometer (EDS, Oxford, UK). The surface compositions were investigated by X-ray photoelectron spectroscopy (XPS, ESCALAB-250).

For measurement of the EM properties, the FeNi@C samples were dispersed in paraffin homogeneously. Then the FeNi@C-paraffin composite was cut into toroidal shape with 7.00 mm outer diameter and 3.04 mm inner diameter. The EM parameters were measured for FeNi@C-paraffin composite containing 40 wt.% FeNi@C, using an Agilent N5244A vector network analyzer (VNA, USA). Coaxial method was used to determine the EM parameters of the toroidal samples in a frequency range of 0.03-18 GHz with a transverse EM mode. The vector network analyzer was calibrated for the full two-port measurement of reflection and transmission at each port. The complex permittivity and complex permeability were calculated from S-parameters tested by the vector network analyzer, using the simulation program of Reflection/Transmission Nicolson-Ross model.[27]

3. Results and Discussion

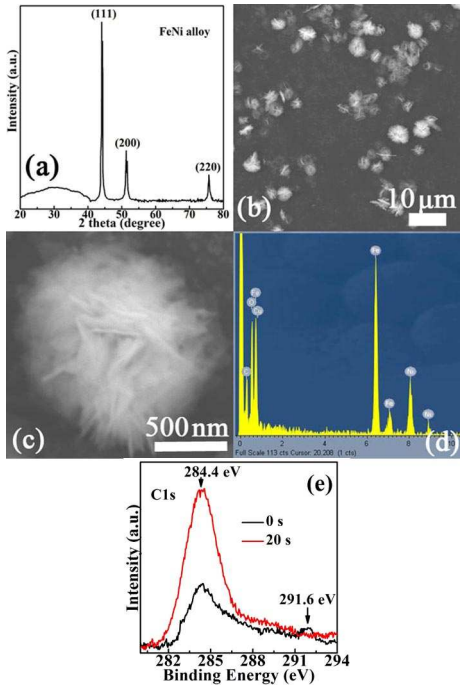

Fig.1 (a) XRD pattern, (b) and (c) SEM images with different magnifications for the flower-like FeNi@C nanocomposites, and (d) EDS image of flower-like FeNi@C nanocomposites. (e) XPS survey patterns for C 1s at the surface for different etching time.

The phase of as-prepared products is confirmed by the XRD as shown in Fig.1(a). The XRD pattern of the as-prepared products shows three distinctive diffraction peaks at 44.06^o, 51.37^o and 75.73^o, corresponding to (111), (200) and (220) planes of FeNi alloy, respectively.[28,29] The result indicates that as-prepared products are the face-centered cubic FeNi alloy. No impurity peak in the XRD pattern reveal that the as-synthesized FeNi alloy has a high degree of purity. The XRD pattern of the carbon displayed a broad peak around 20^o-40^o indicating the presence of a non-crystalline material. Similar XRD patterns (20^o-40^o) have been observed for amorphous carbon and carbon-coated Cu nanoparticles.[30,31] Fig.1 (b) and (c) demonstrate the SEM images of the products with different magnifications. The as-synthesized products presents the flower-like microstructure

with a diameter of 0.5-4 μm, as seen from Fig.1(b). Furthermore, the magnified SEM images (Fig.1(c)) demonstrate that three-dimensional flower-like microstructures are self-assembled by lots of nanosheets building blocks with the thickness ranging between 10 and 80 nm. There are some flocculent structures between the nanosheets, which are determined to be carbon by EDS. It is worthwhile noting that the as-obtained flower-like FeNi@C microstructures cannot be destroyed and broken into the individual FeNi nanosheets even after subjecting long-time ultrasonication. The forces binding them together maybe include magnetic forces among FeNi nanosheets and the binding forces from the flocculent carbon. The chemical composition of the flower-like FeNi@C microstructures is further confirmed by EDS as shown in Fig.1 (d). The existence of Cu is ascribed to the conducting glue and supporter. From the peak intensity in EDS, the atomic percentage of Fe is measured to be 49.2 %, close to the theoretical value of 50% calculated by the content of the precursor. Fig.1(e) shows the binding energy of C 1s electrons in the nanocomposites. The peak at 284.4 eV belongs to 1s electrons of the flocculent carbon and the peak at 291.6 eV to 1s electrons of CO_2.[32,33] The peak at 291.6 eV disappears when the etching time reaches up to 20 s, indicating the CO_2 on the surface of nanocomposites is from the ambience.

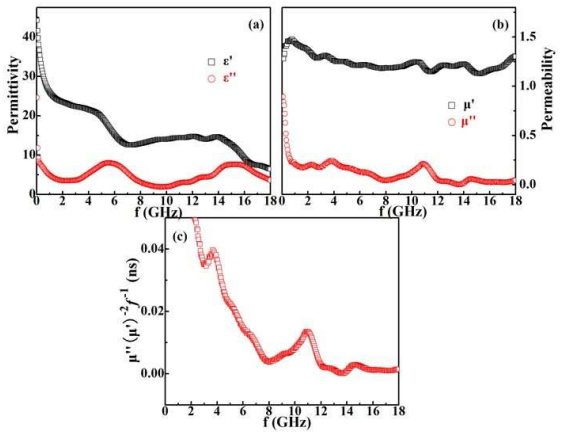

Fig.2 Frequency dependence of (a) the relative complex permittivity and (b) the relative complex permeability, and (c) frequency dependence of $\mu''(\mu')^{-2}f^{-1}$

The EM parameters of FeNi@C nanocomposites are mainly dictated by its permittivity (ε_r) and permeability (μ_r) (in the measurement, the FeNi@C nanocomposites are mixed with paraffin, so the EM properties can be regarded as the properties belonging to FeNi@C-paraffin composite), which are measured at room temperature for the investigation of EM absorption properties of nanocomposites. The frequency dependencies of the real part (ε') and the imaginary part (ε'') of the complex permittivity (ε_r) are shown in Fig.2 (a). Both ε' and ε'' are found to decrease with increasing frequency due to an increased lagging behind of dipole-polarization response with respect to the electric-field change.[1] Two maxima are observed in ε'' around 5.55 and 15.26 GHz. As known, the ε' and ε'' represent the polarization and the dielectric loss, respectively. One peak may result from the relaxation loss of permanent electric dipoles due to the amorphous C. The other peak may be attributed to the relaxation loss of interfacial polarization of the heterogeneous system due to the electronegativity difference between the FeNi and C.[1,9]

In the metal-based composites, two kinds of mechanisms for the polarization phenomena could be used to explain the frequency dependency of permittivity. The first mechanism is the space charge polarization, which occurs between adjacent conductive metal particles and contributes to a high dielectric constant. With respect to the micro-composites, the nano-sized metallic particles in nanocomposites are weak on the metallic behavior. As a result, the space charge polarization is weaken in the nanocomposites, resulting in the relatively low permittivity of flower-like FeNi@C nanocomposites. The second mechanism of polarization is the dipole polarization. The nanocomposite is such a perfect system, because the polarized metal cores can play the role of dipoles, especially at a high frequency, as demonstrated in the Fe or Ni nanoparticles. Considering the microstructure in flower-like FeNi@C nanocomposites, it is reasonable that the dipole polarization is the dominant at higher frequency and the weak space charge polarization mainly works at lower frequency.[9]

Fig.2 (b) shows the changes with frequency in the real part (μ') and imaginary part (μ'') of the complex permeability (μ_r) for composite. As shown in Fig.2(b), μ' increases in frequency from 0.03-0.79 GHz and then exhibits the concussive increase with increasing frequency, which is similar with the previous report.[34] The μ' exhibits a significant fluctuation from 1.46 to 1.13 over the 0.79 -18 GHz, which is bigger than spherical-like nanocomposites.[1-3,9-15] Generally, μ'' represents magnetic energy dissipation, and a resonance peak of μ'' at a certain frequency refers to a high magnetic loss thereat.[3] It is clearly observed that four peaks appear at 2.23, 3.94, 10.86 and 14.63 GHz on μ'' curve, indicating the strong magnetic loss in the present composite. Furthermore, magnetic loss is caused by the time lag of the magnetization vector **M**, behind the magnetic field vector **H**. The change of the magnetization vector **H** is generally brought about by rotation of the magnetization or the domain wall displacement. In the high frequency range, the motion of the magnetization vector **M** cannot keep up with the applied field, which results in the occurrence of μ''.[35] Generally, the microwave magnetic loss of magnetic composites can be explained by hysteresis loss, domain-wall resonance, eddy current effect, natural resonance and exchange resonance for particles smaller than 100 nm. The hysteresis loss can be excluded because the applied microwave field is weak. The domain-wall resonance usually occurs below the gigahertz range. For the ferromagnetic absorber, the EM absorption properties are usually subject to degradation caused by the eddy current effect in the high-frequency region. The eddy current losses can be expressed by $\mu''(\mu')^{-2}f^{-1} = 2\pi\mu_0 d^2\sigma/3$, where σ, d and μ_0 are the electric conductivity, the thickness of the absorber and the permeability in vacuum, respectively . If the magnetic loss results only from eddy current loss, the values of $\mu''(\mu')^{-2}f^{-1}$ should are constant with different frequencies.[36] Fig.2 (c) shows the frequency as a function of $\mu''(\mu')^{-2}f^{-1}$. From Fig.2(c), it can be seen that there are double-peaks in $\mu''(\mu')^{-2}f^{-1}$ -f curve. The difference

of $\mu''(\mu')^{-2}f^{-1}$values is larger than 0.05 ns, indicating the eddy current loss is suppressed effectively and the eddy current loss is not the dominant magnetic loss in the 0.03-18 GHz frequency range.[37,38] As reported elsewhere,[3,34,39] the resonance peaks of μ'' at 2.23 and 3.94 GHz are mainly attributed to the natural resonance originated from traditional static magnetic energy, the ones at 10.86 and 14.63 GHz are the exchange resonance frequencies since the FeNi@C nanosheet size is small enough to result in the occurrence of exchange resonance. Thus, the magnetic loss in the FeNi@C nanocomposites arises from the natural resonance and exchange resonance. It is believed that coexistence of natural resonance and exchange resonance can result in strong magnetic loss, implying enhanced microwave absorption by the FeNi@C nanocomposites as EM energy is converted into heat energy.[3,39]

With the purpose of charactering the microwave absorption properties, the representation reflection loss (RL) of the composites at different sample thickness are simulated, as shown in Fig.3 (a), by using the measured complex permittivity and permeability based on the transmit-line theory with the following equations:

$$Z_{in} = Z_0(\mu_r/\varepsilon_r)^{1/2}\tanh[j(2\pi fd/c)(\mu_r\varepsilon_r)^{1/2}]$$

$$RL = 20\lg|(Z_{in}-Z_0)/(Z_{in}+Z_0)|$$

Where f is the frequency of the EM wave, d is the thickness of the absorber, c is the velocity of light, Z_0 is the impedance of air, and Z_{in} is the input impedance of the absorber. The dip in RL indicates the occurrence of absorption or minimal reflection of the microwave power.[27]

Fig.3 (a) shows that the peak of RL is found to sensitively depend on the sample thickness, and the strong peak position of RL shifts to lower frequency range with increasing the thickness, and the amplitudes of RL increase first, and decrease then, and keep a similar constant afterwards. The above similar phenomena have been reported in the CoNi@C absorber.[37] As is shown in Fig.3(a), it is clearly noted that an optimal RL of -46.7 dB, corresponding to 99.998 % absorption, is observed at 3.17 GHz for 4.4 mm thickness layer. The absorbent with a thickness of 1.3 mm has a RL value of -32.78 dB at 13.78 GHz. It can been seen from Fig.3(a) that two dips appear simultaneously when the thickness of the composite exceeds a certain value (3.5) and three dips exist in the RL-f curves when the thickness is over 5.8 mm.

When an EM wave is incident on an absorber sample backed by a metal plate, it is partially reflected from air to absorber interface and partially reflected from absorber to metal interface. At some special frequency point, these two reflected waves are out of phase by 180° and cancel each other for the thickness of absorber satisfying the quarter-wave thickness criteria, which means the peak frequency dependence of the RL for the ferromagnetic metal based composite complies with the quarter-wavelength matching model:[21]

$$t_m = \frac{n}{4}\lambda_m = \frac{nc}{4f_m\sqrt{|\varepsilon_r\mu_r|}}(n=1,3,5.....)$$

Where f_m is the peak frequency of RL, tm is the thickness of the sample, ε_r and μ_r are the complex permittivity and permeability at f_m, respectively. According to this model, the peak frequency is inversely proportional to the thickness.

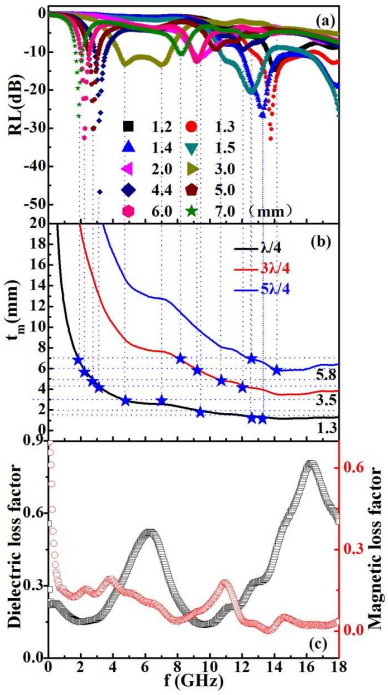

Fig.3 (a) Dependence of RL on frequency at typical thicknesses and (b) dependence of λ/4, 3λ/4 and 5λ/4 on frequency for the flower-like FeNi@C-paraffin composite from its complex permeability and permittivity with frequency. The vertical dot lines are extended from the RL peaks in (a), each line from the RL peak under an absorber thickness crosses with its corresponding thickness contour in (b). The crossover points are indicated by the asteroid dots. (c) Dielectric loss factor and magnetic loss factor as a function of frequency for the flower-like FeNi@C-paraffin composite.

In order to verify the possibility of employing the quarter-wavelength matching model to fit the frequency dependence of dips in RL for FeNi@C-paraffin composite, Fig.3(b) gives the dependence of λ/4, 3λ/4 and 5λ/4 on frequency for the FeNi@C-paraffin composite. In Fig.3(a), the vertical dot lines are extended from the RL peaks, and each line from the RL peak under an absorber thickness crosses with its corresponding thickness contour in Fig.3(b). The crossover points are indicated by the asteroid dots.

There are two possible contributions for microwave absorption, namely, dielectric loss and magnetic loss.[36] We have also calculated both the dielectric loss factor ($\tan(\delta_\varepsilon)=\varepsilon''/\varepsilon'$) and the magnetic loss factor ($\tan(\delta_\mu)=\mu''/\mu'$) based on the permeability and permittivity of the composite measured as shown in Fig. 2(a) and 2(c). Fig. 3(c) shows the dielectric loss factor exhibit the broad peaks at around 6.20 and 16.18 GHz, and the magnetic loss factor exhibit the peaks at around 2.22, 3.78, 10.91 and 14.48 GHz, indicating that the FeNi@C-paraffin composite may possess the enhanced EM absorption abilities in the above peak frequency range.

The following information in 0.03-18 GHz range can be obtained from the thickness contours in Fig. 3(b): (1) when the absorber thickness t≤1.3 mm, the thickness is too thin to the

quarter-wavelength cancellation condition. The frequency of RL peak exists in the natural frequency of dielectric loss factor and magnetic loss factor range. The RL peaks are ascribed to the synergy of dielectric loss and magnetic loss; (2) when the absorber thickness t > 1.3 mm, for almost RL peaks for any thickness, the almost thickness contour has crossover points with the λ/4, 3λ/4 and 5λ/4 curves, indicating the frequency of RL peak are determined by the quarter-wavelength cancellation condition. In addition, it is worthy noted that the RL peak exists at 7 GHz for the absorber thickness with 3.0 mm, which the thickness contour has no crossover point with the λ/4 curve. On based on the Fig.3(a)-(c), the RL peak at 7 GHz are described to the synergy of dielectric loss and magnetic loss. The composite should have large imaginary parts of the permittivity or permeability at microwave frequency to significantly absorb the EM wave energy, which is now in the material. This is called the EM loss model. However, the peak frequency dependence of RL complies with the quarter-wavelength matching model for the almost dips when the absorber thickness t > 1.3 mm. This means that the energy loss of EM wave results from the interface loss and the EM loss simultaneously.

Conclusions

Flower-like FeNi@C nanocomposites have been synthesized via a hydrothermal method. Flower-like FeNi@C nanocomposites with a diameter of 0.5-4 μm are self-assembled by the FeNi nanosheets with the thickness ranging between 10 and 80 nm and flocculent carbon between FeNi nanosheets. The EM properties of FeNi@C nanocomposites have been investigated in detail. Due to a cooperative consequence of the FeNi-C interfaces and the dielectric carbon, dual dielectric relaxations exist in the present system. The coexistence of natural resonance and exchange resonance result in strong magnetic loss. For 4.4 mm thickness layer, an optimal RL of -46.7 dB is observed at 3.17 GHz. The absorbent with a thickness of 1.3 mm has a RL of -32.78 dB at 13.78 GHz. The enhanced EM absorption abilities result from the synergy of dielectric loss and magnetic loss and the quarter-wavelength cancellation simultaneously. The flower-like FeNi@C nanocomposites can be a potential material for fabricating microwave devices.

Acknowledgements

This study has been supported by the National Natural Science Foundation of China (Grant No. 51201002).

Notes and references

[a]*School of Materials Science and Engineering, Anhui University of Technology, Maanshan,243002, China. Fax:+86 555 2311570; Tel: +86 555 2311570; E-mail: liuxianguohugh@gmail.com*
[b]*Center for Engineering practice and Innovation Education, Anhui University of Technology, Maanshan,243032, China.*

† Electronic Supplementary Information (ESI) available: See DOI: 10.1039/b000000x/

1 H. Wang, H.H. Guo, Y.Y. Dai, D.Y. Geng, Z. Han and D. Li, Appl. Phys. Lett. 2012, 101, 083116.
2 X.F. Zhang, P.F. Guan and X.L. Dong, Appl. Phys. Lett. 2010, 97, 033107.
3 S.H. Pan, X.Q. Cheng, C.H. Zhang, C.H. Gong, L.G. Yu and J.W. Zhang, Appl. Phys. Lett. 2013, 102, 012410.
4 Q.C. Liu, Z.F. Zi, M. Zhang, P. Zhang, A.B. Pang and J.M. Dai, J. Mater. Sci. 2013, 48, 6048-6055.
5 R.B. Yang, W.F. Liang, C.W. Lou and J.H. Lin, J. Appl. Phys. 2012, 111, 07A338.
6 P.F. Guan, X.F. Zhang and J.J. Guo, Appl. Phys. Lett. 2012, 101, 153108.
7 R.K. Srivastava, T.N. Narayanan, A.P.R. Mary, M.R. Anantharaman, A. Srivastava and R. Vajtai, Appl. Phys. Lett. 2011, 99, 113116.
8 R.C. Che, L.M. Peng, X.F. Duan, Q. Chen and X.L. Liang, Adv. Mater. 2004, 16, 401-405.
9 B. Lu, X.L. Dong, H. Huang, X.F. Zhang, X.G. Zhu and J.P. Sun, J. Magn. Magn. Mater. 2008, 320, 1106-1111.
10 X.G. Liu, Y.P. Sun, C. Feng, C.G. Jin and W.H. Li, Appl. Surf. Sci. 2013, 280, 132-137.
11 X.G. Liu, Z.Q. Ou, D.Y. Geng, Z. Han, Z.G. Xie and Z.D. Zhang, J. Phys. D: Appl. Phys. 2009, 42, 155004.
12 X.G. Liu, D.Y. Geng, S. Ma, H. Meng, M. Tong and D.J. Kang, J. Appl. Phys. 2008, 104, 064319.
13 Z.H. Wang, X. He, X. Wang, Z. Han, D.Y. Geng and Y.L. Zhu, J. Phys. D: Appl. Phys. 2010, 43, 495404.
14 X.F. Zhang, X.L. Dong, H. Huang, B. Lv, J.P. Lei and C.J. Choi, J. Phys. D: Appl. Phys. 2007, 40, 5383-5387.
15 X.G. Liu, S.W. Or, S.L. Ho, C.C. Cheung, C.M. Leung and Z. Han, J. Alloys Compd. 2011, 509, 9071-9705.
16 J.Q. Wei, T. Wang and F.S. Li, J. Magn. Magn. Mater. 2011, 323, 2608-2612.
17 L.G. Yan, J.B. Wang, X.H. Han, Y. Ren, Q.F. Liu and F.S. Li, Nanotechnology 2010, 21, 095708.
18 S.S. Kim, S.T. Kim, Y.C. Yoon and K.S. Lee, J.Appl. Phys. 2005, 97, 10F905.
19 T.D. Zhou, J.K. Tang and Z.Y. Wang, J. Magn. Magn. Mater. 2010, 322, 2589-2592.
20 J.Q. Wei, Z.Q. Zhang, B.C. Wang, T. Wang and F.S. Li, J. Appl. Phys. 2010, 108, 123908.
21 T. Wang, R. Han, G.G. Tan, J.Q. Wei, L. Qiao and F.S. Li, J. Appl. Phys. 2012, 112, 104903.
22 S. Bai, X.P. Shen, G.X. Zhu, Z. Xu and J. Yang, CrystEngComm, 2012, 14, 1432-1438.
23 Q.L. Liao, R. Tannenbaum and Z.L. Wang, J. Phys. Chem. B 2006, 110, 14262-14265.
24 X.G. Liu, S.W. Or, Y.P. Sun, W.H. Li, Y.Z. He and G.H. Zhu, J. Alloys Compd. 2013, 548, 239-244
25 M.S. Cao, J. Yang, W.L. Song, D.Q. Zhang, B. Wen and H.B. Jin, ACS Appl. Mater. Interfaces 2012, 4, 6949-6956.
26 X.G. Liu, S.W. Or, C.G. Jin, Y.H. Lv, W.H. Li and C. Feng, Carbon 2013, 60, 215-220.
27 X.G. Liu, C. Feng, S.W. Or, C.G. Jin, F. Xiao and A. L. Xia, Mater. Res. Bull. 2013, 48, 3887-3891.
28 Y.Y. Sun, Q. Liang, Y.J. Zhang, Y. Tian, Y.Q. Liu and F.X. Li, J. Magn. Magn. Mater. 2013, 332, 85-88.
29 L.J. Liu, J.G. Guan, W.D. Shi, Z.G. Sun and J.S. Zhao, J. Phys. Chem. C 2010, 114, 13565-13570.
30 D.J. Guo and H.L. Li, Carbon 2005, 43, 1259-1264.
31 E.K. Athanassiou, R.N. Grass and W.J. Stark, Nanotechnology 2006, 17, 1668-1673.
32 C.J. Powell, J. Electron Spectrosc. Relat. Phenom 2012,185, 1-3.
33 U. Gelius, P.F. Heden, J.Hedman, B.J. Lindberg and K. Siegbahn, Phys. Scripta 1970, 2, 70-74.
34 L.J. Deng, P.H. Zhou, J.L. Xie and L. Zhang, J. Appl. Phys. 2007, 101, 103916.
35 X.G. Liu, B. Li, D.Y. Geng, W.B. Cui, F. Yang and Z.D. Zhang, Carbon 2009, 47, 470-474.
36 C.L. Zhu, M.L. Zhang, Y.J. Qiao, G. Xiao, F. Zhang and Y.J. Chen, J. Phys. Chem. C 2010, 114, 16229-16235.
37 S.J. Yan, C.Y. Xu, J.T. Jiang, D.B. Liu, Z.Y. Wang and J. Tang, J. Magn. Magn. Mater. 2014, 349, 159-164.
38 W.W. Pan, Q.F. Liu, R. Han, X. Chi and J.B. Wang, Appl. Phys. A 2013, 113, 755-761.
39 Y.P. Sun, X.G. Liu, C. Feng, J.C. Fan, Y.H. Lv and Y.R. Wang, J. Alloys Compd. 2014, 586, 688-692.

Color graphic

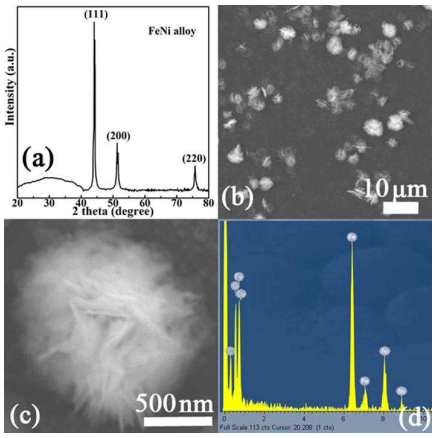

The flower-like FeNi@C nanocomposites can be a potential material for fabricating microwave devices.